Solar Energy
And Sustainable Development
Refereed, biannual scientific journal issued by:
The Libyan Center for Solar Energy Research and Studies

Modified-TiO_2 Nanotube Arrays as a Proficient Photo-Catalyst Nanomaterial for Energy and Environmental Applications

Riyadh Ramadhan Ikreedeegh[1,2,3*], Muhammad Tahir[1], Mohamed Madi[4].

[1]Chemical and Petroleum Engineering Department, UAE University, P.O. Box 15551, Al Ain, United Arab Emirates.

[2]Department of Analysis and Quality Control, Sarir Oil Refinery, Arabian Gulf Oil Company, El Kish, P.O. Box 263, Benghazi, Libya.

[3]Libyan Advanced Center for Chemical Analysis, Libyan Authority for Scientific Research, Tripoli, Libya.

[4]Chemical Engineering Department, Higher Institute for Science and Technology, Souk Al-Khamis, Libya.

E-*mail:* riyadhkridiegh@gmail.com , muhammad.tahir@uaeu.ac.ae .

ARTICALE INFO.

Article history:
Received 12 Mar 2024
Received in revised form 15 Mar 2024
Accepted 6 May 2024
Available online 10 May 2024

KEYWORDS

TiO_2 nanotube arrays, Photocatalysis,CO_2 reduction, CH_4 production, Solar fuels.

ABSTRACT

Recently, TiO_2 nanotube arrays (TNTAs) have attracted researcher's attention in the fields of energy production and environmental remediation applications; this is mainly due to their unique optoelectronic characteristics, corrosion resistance, chemical and mechanical stability. In this study, the ability of employing of TiO_2 nanotube arrays-based catalysts in the field of photocatalytic CO_2 reduction has been investigated. Possible modification strategies have been presented for improving the TNTAs performance by using different types of nanomaterials including graphitic carbon nitrides (g-C_3N_4), metal-organic frame work (MOF), reduced graphene oxide (RGO) and gold nanoparticles (Au NPs).

The TNTAs composites were characterized using XRD and FESEM analyses and the results revealed the successful synthesis of these composites. The TNTAs and their composites exhibited good results for the photo-conversion of CO_2 into CH_4 gas product. This study gives new ideas for making and developing low-cost Ti metal-based nanomaterials which can be used in the future for recycling the CO_2 gas emissions into useful solar fuels.

*Corresponding author.

DOI: https://doi.org/10.51646/jsesd.v13i1.196

مصفوفات أنابيب ثاني أكسيد التيتانيوم النانوية المُعدلة كمُحفز ضوئي نانوي فعال لتطبيقات الطاقة والبيئة

رياض رمضان كريديغ ، محمد طاهر، محمد مادي .

ملخص: في الآونة الأخيرة، جذبت مصفوفات أنابيب ثاني أكسيد التيتانيوم النانوية (TNTAs) إهتمام الباحثين في مجالات إنتاج الطاقة وتطبيقات المعالجة البيئية. ويرجع ذلك أساسًا إلى خصائصها الإلكترونية البصرية الفريدة، ومقاومتها للتآكل، وثباتها الكيميائي والميكانيكي. في هذه الدراسة تم دراسة إمكانية استخدام بعض المُحفزات المعتمدة على مصفوفات أنابيب ثاني أكسيد التيتانيوم النانوية في مجال اختزال ثاني أكسيد الكربون بالتحفيز الضوئي. تم تقديم استراتيجيات التعديل الممكنة لتحسين أداء الTNTAs باستخدام أنواع مختلفة من المواد النانوية بما في ذلك نيتريدات الكربون الجرافيتية ($g\text{-}C_3N_4$) والهياكل الفلزية العضوية (MOFs) وأكسيد الجرافين المخفض (RGO) والجسيمات النانوية الذهبية (Au NPs). تم تشخيص مركبات الـ(TNTAs) باستخدام تحليلات XRD وFESEM وكشفت النتائج عن نجاح تصنيع هذه المركبات. أظهرت الـ(TNTAs) ومركباتها نتائج جيدة للتحويل الضوئي لغاز ثاني أكسيد الكربون إلى منتج غاز الميثان CH_4. تقدم هذه الدراسة أفكارًا جديدة لصنع وتطوير مواد نانوية منخفضة التكلفة تعتمد على معدن التيتانيوم والتي يمكن استخدامها في المستقبل لإعادة تدوير انبعاثات غاز ثاني أكسيد الكربون إلى وقود مُفيد.

الكلمات المفتاحية – مصفوفات أنابيب ثاني أكسيد التيتانيوم النانوية، التحفيز الضوئي، تقليل ثاني أكسيد الكربون، إنتاج الميثان، الوقود الشمسي.

1. INTRODUCTION

The ever-increasing demand on fossil fuels has led to a severe shortage in these resources and will result in a global energy crisis in the near future [1, 2]. Moreover, burning of these fuels generates massive amounts of greenhouse gases, particularly CO_2, which is considered as the primary cause of many environmental issues including climate change, sea level rise, acid rains and losses of biodiversity [3, 4]. Recently, a new technology known as photocatalysis has been introduced as one of the main promising solutions for addressing all the above mentioned problems [5]. This technology is considered as a photochemical process that utilizes solar light energy for the conversion of CO_2 into valuable chemical and fuels in the presence of a semiconductor material named as a photocatalyst. This photocatalyst is considered as the most important element in this process. Among all the metal oxide materials, TiO_2 has been widely used as one the benchmark photocatalysts in many fields of CO_2 reduction [6, 7], hydrogen production [8, 9] and pollutants degradation [10, 11] and other applications. This is mainly due to its wide advantages including low cost, availability, non-toxicity, corrosion resistance, high thermal and chemical stability [12, 13]. However, the TiO_2 still have some issues related to light absorption and high recombination of photo-generated charge carriers [14].

Recently, TiO_2 in the form of nanotube arrays (TNTAs) has attracted researcher's attention due to its vertical hierarchical structure offering larger internal surface area with enhanced transfer of charge carriers [15]. Although TNTAs exhibit higher surface area and long-term charge mobility compared to other traditional TiO_2 nanostructures, they are still being active only at UV light and suffers from the charges recombination [16]. Huge efforts have been devoted to enhance the photocatalytic performance of TNTAs through different modification strategies such as doping with organic materials [9, 17], incorporation and coupling with noble metals [18, 19].

In this study, a simple electrochemical anodization method has been used for the fabrication of TiO_2 in the form of nanotube arrays (TNTAs). Then, the TNTAs photocatalyst was characterized using XRD and FESEM analyses and then investigated for its ability for the conversion of CO_2 gas in to methane gas (CH_4) under visible light. Finally, a comparative study was conducted

for investigating the effect of modifying the TNTAs using various materials including graphitic carbon nitrides (g-C_3N_4), NH_2-MIL-125(Ti) MOF, reduced graphene oxide (RGO) and gold nanoparticles (Au NPs) based on both characterization analyses and experimental work.
This study provides a step forward towards better understanding for the fabrication and development of proficient and low-cost nanomaterial composites for the applications of energy productions and environmental remediation.

2. EXPERIMENTAL SECTION

2.1. Chemicals and Reagents

All chemicals used in this study were of analytical grade and were used as received without further purification. To prepare TNTAs, titanium metal sheets (Sigma Aldrich, 99.7%), platinum metal foils (Sigma Aldrich, 99.7%), ethylene glycol (Sigma Aldrich, 99.5%), ammonium fluoride (QREC, 98%), methanol (Merck, 99.9%), ethanol (Merck, 99.9%) and distilled water were used. However, the following chemicals were used for preparing the modification composites: titanium isopropoxide (99.9%, Sigma Aldrich), 2-aminoterephthalic acid (99%, Sigma Aldrich) and DMF (Merck, 99.9%) for preparing MOF. Melamine (Merck, 99.99%) for preparing g-C_3N_4. Graphite flakes (Sigma Aldrich, 99.9%), potassium permanganate (Sigma Aldrich 99%), Sulphuric acid (Sigma Aldrich 97%) and phosphoric acid (Merk, 99%) for preparing RGO. Gold(III) chloride hydrate (Sigma Aldrich, 99.99%) for preparing Au.

2.2. Preparation of TNTAs

The TNTAs layer was formed over the Ti metal sheet using an electrochemical anodization method similar to previous studies [20, 21]. Prior to the anodization process, the Ti metal sheet (4 cm × 2.5 cm, 0.25 mm thick) was polished, rinsed and sonicated in three different solvents of ethanol, methanol and distilled water, respectively.
The electrochemical anodization process was conducted by employing the Ti sheet as a working electrode (anode) and a Pt sheet as a counter electrode (cathode) in an ethylene glycol-based electrolyte solution consisting of 100 mL of ethylene glycol (EG), 1.12 g of ammonium fluoride (NH_4F) and 2 mL of distilled water.
This process continued for 4 h at room temperature and under a constant voltage of 30 V supplied by a DC power source. The anodized Ti sheet was then rinsed with distilled water, dried and annealed at 550 °C for 2 h in a programmable furnace for obtaining highly ordered TiO_2 nanotube arrays.

2.3. Preparation of TNTAs/g-C_3N_4 composite

Firstly, the g-C_3N_4 was prepared through a calcination process of pure melamine powder as reported in our previous works [5, 22]. The melamine powder was heated in a muffle furnace for 2 h at 550 °C. Then, the obtained yellow powder was collected, cooled to room temperature and crushed in to fine powder. The g-C_3N_4 powder (0.1 g) was dispersed in a methanol solution (50 mL) for producing a pure structure of g-C_3N_4 nanosheets. Finally, the as-prepared TNTAs were immersed in this solution under ultrasonic treatment for 15 min and then dried in oven at 100 °C for 12 h to obtain the TNTAs/g-C_3N_4 nanocomposite.

2.4. Preparation of TNTAs/NH_2-MIL-125(Ti) MOF composite

A solvothermal method was used to prepare the NH_2-MIL-125(Ti) MOF as reported in previous studies [23, 24]. Briefly, specific amounts of 2-amino terephthalic acid (1.0869 g) and titanium

isopropoxide (0.4263 g) were added to a 20 mL DMF/methanol solution (v/v = 9:1). The mixture was stirred for 30 min, then transferred to a Teflon-lined autoclave to be hydrothermally treated for 72 h at 150 °C. The resultant yellow suspension was then cooled, filtered, washed 3 times with DMF and methanol, respectively and dried in oven for 12 h at 80 °C to obtain a yellow fine powder. Finally, the TNTAs sample was immersed in a methanol solution of the obtained MOF powder (0.1 g MOF in 50 mL methanol) and dried at 100 °C for 12 h

2.5. Preparation of TNTAs/RGO composite

Natural graphite flakes were oxidized to prepare graphene oxide (GO) through a modified Tour's method [22, 25].

The oxidation of graphene was achieved by adding a certain amount of graphite (3 g) to a mixed solution of H_2SO_4 (360 mL) and H_3PO_4 (40 mL) with continuous stirring at 300 rpm and a constant temperature of 10 °C. $KMnO_4$ (18 g) was then added gradually so that the temperature of the solution is kept under 50 °C. A yellow suspension was obtained after 24 h of stirring which was then cooled and altered using H_2O_2 (5 mL) until a brown color is obtained.

The suspension was then filtered, washed with distilled water, ultrasonicated and dried at 50 °C for 12 h for delivering exfoliated single-layer GO nanosheets. However, the RGO was simply prepared by heating the GO powder for 3 min at 300 °C. The RGO-TNTAs composite was fabricated by immersing the pure TNTAs sample in a prepared RGO mixture (0.5 mg/L) under ultrasonication for 20 min.

Finally, the TNTAs sample was dried at 60 °C for 5 h.

2.6. Preparation of TNTAs/Au composite

The Au nanoparticles were successfully deposited on the surface of TNTAs using a simple electrochemical deposition method similar to the previously reported studies [26, 27]. Briefly, a Ti foil was employed as an anode while the as-prepared TNTAs sample was utilized as a cathode in an ethylene glycol electrolyte (125 mL) containing $HAuCl_4$ (0.125 g). The electrochemical process was conducted for 3 min under a voltage of 4 V and at a temperature of 25 °C. The sample was then cleaned with distilled water, dried and annealed at 550 °C for 2 h to obtain well-ordered, Au-deposited TNTAs.

2.7. Photocatalyst Characterizations

The prepared samples were characterized using both X-ray diffraction (XRD) patterns and Field Emission Scanning Electron Microscopy (FESEM) images. A D8 Bruker diffractometer was employed for obtaining the XRD patterns for investigating the crystalline phases and crystals structure of the prepared samples while a Hitachi SU8020 FESEM microscope was used to study the surface morphologies of the samples in this study.

2.8. Photocatalytic performance and reactor set-up

A stainless steel reactor equipped with a quartz glass window, Xe lamp, inlet and outlet valves was employed for investigating the photocatalytic CO_2 reduction performance of the prepared samples.

Prior to the photo-reaction, the system was purged with N_2 gas for the removal of any other gases. Then a purified CO_2 gas was fed to the system after being passed in a water bubbler for carrying the H_2O molecules with the CO_2 gas.

The CO_2 reduction process was started after switching on the light source and continued for 4 h. However, a gas sample was drawn using a gas syringe through the sample point and injected to a gas chromatograph (Agilent GC 6890 N, USA) for analyzing the methane amounts. Figure 1

illustrates the whole reactor set-up used for the photo-conversion of CO_2 gas into CH_4.

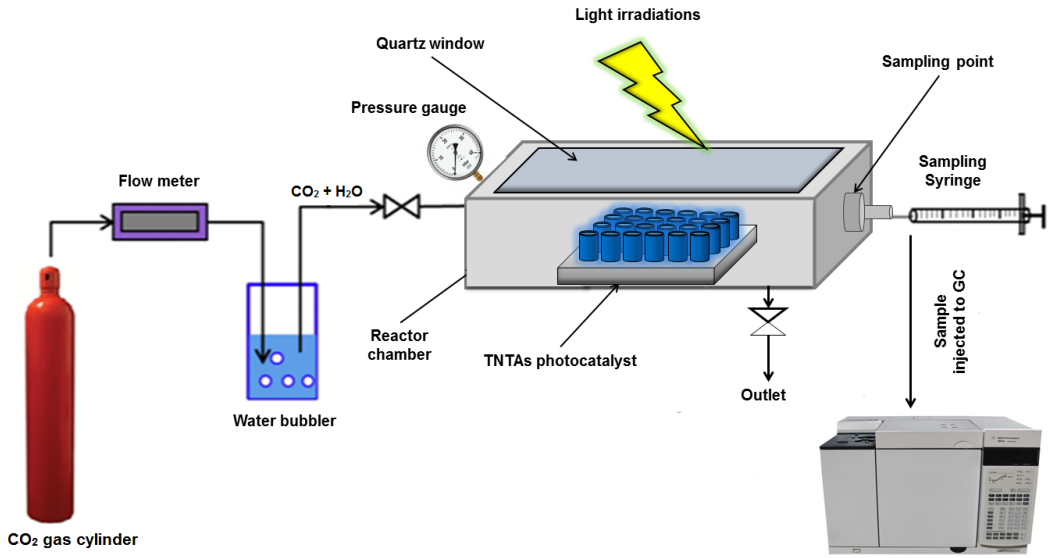

Figure 1. The photo-reactor set-up used for the conversion of CO_2 into CH_4 under visible light.

3. RESULTS AND DISCUSSION

3.1. Characterization

3.1.1. X-ray Diffraction (XRD) Analysis

Figure 2 shows the XRD patterns of pure TNTAs, modification composites and modified TNTAs. The pure TNTAs displayed several peaks of TiO_2 anatase phase at 2θ: 25.27°, 37.7°, 48.1°, 55.1°, 62.5°, corresponding to the (101), (004), (200), (211) and (204) crystallographic planes, respectively (JCPDS card No. 21–1272) [28-30] in addition to the rutile phase at 2θ: 27.3°, 36.09°, 54.2°, 69.1°, attributed to the crystal planes of (110), (101), (105) and (301), respectively (JCPDS card No. 21–1276) [29, 31]. The g-C_3N_4 appeared with its prominent diffraction peaks at 2θ: 12.8° and 27.3°, which are indexed to the (100) and (002) lattice planes of g-C_3N_4 (JCPDS No.87–1526), respectively [32, 33]. Both peaks were also appeared in the TNTAs/g-C_3N_4 sample. The RGO exhibited a broad peak at 2θ: 23.7° and a small peak at 2θ: 42.7° which can be attributed to the (002) and (111) RGO diffraction planes, respectively, [34, 35].

However the RGO peaks did not show in the TNTAs/RGO since they might be overlapped with the TNTAs peaks. The XRD pattern of pure MOF displayed strong diffraction peaks at 6.7° (101), 9.7° (200), 11.5° (211), 16.6° (222) and 17.9° (312) which are in agreement with the previously reported studies [23, 36, 37].

Clearly, all MOF peaks were also appeared in the TNTAs/MOF sample. It is worth mentioning that no peaks were shown for the TNTAs/Au composite which might be attributed to the low content of Au in the binary composite.

Table 1 summarizes all the XRD diffraction peaks of the tested samples with their ascribed positions and other relevant details.

Table 1. The samples XRD diffraction peaks with their ascribed positions and other relevant details.

Sample	Diffraction Peak	Position (2θ)	Phase	JCPDS card No.
TNTAs	(101)	25.27°	Anatase	21-1272
TNTAs	(004)	37.7°	Anatase	21-1272
TNTAs	(200)	48.1°	Anatase	21-1272
TNTAs	(211)	55.1°	Anatase	21-1272
TNTAs	(204)	62.5°	Anatase	21-1272
TNTAs	(110)	27.3°	Rutile	21–1276
TNTAs	(101)	36.09°	Rutile	21–1276
TNTAs	(105)	54.2°	Rutile	21–1276
TNTAs	(301)	69.1°	Rutile	21–1276
g-C_3N_4	(100)	12.8°	-	87-1526
g-C_3N_4	(002)	27.3°	-	87-1526
g-C_3N_4	(002)	23.7°	-	87-1526
RGO	(111)	42.7°	-	26-1080
RGO	(101)	6.7°	-	26-1080
MOF	(200)	9.7°	-	-
MOF	(211)	11.5°	-	-
MOF	(222)	16.6°	-	-
MOF	(312)	17.9°	-	-

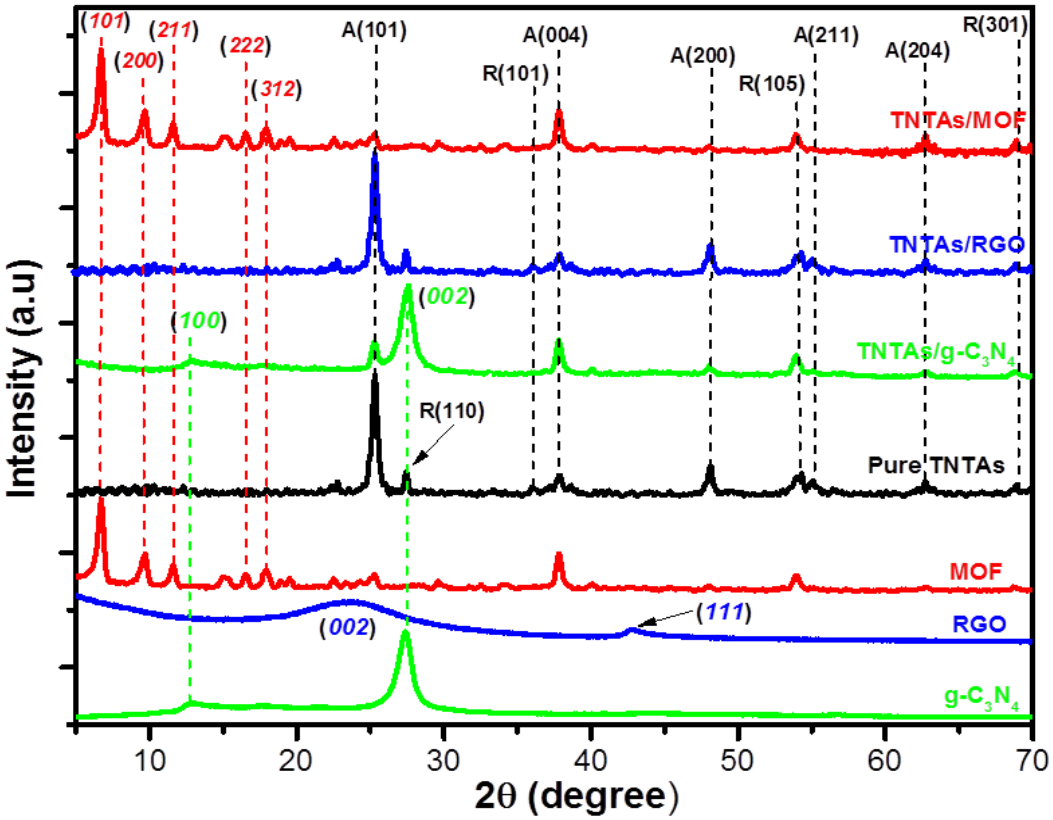

Figure 2. XRD patterns of pure and modified TNTAs samples.

3.1.2. Field Emission Scanning Electron Microscopy (FESEM)

Figure 3 (a-e) shows the FESEM images of pure TNTAs, g-C_3N_4, MOF, RGO and Au, respectively. The top view image of TNTAs sample in Figure 3 (a) shows hierarchical, clean and open-pores TiO_2 nanotubes with average inner diameter of about 90 nm and tube length reaching up to 5µm. In Figure 3 (b), the graphitic carbon nitrides displayed a layered compact nanosheet structure. Similar to g-C_3N_4, the RGO sample displayed large nanosheet structure reaching up to 10 µm in length as shown in (Figure 3 (d)). However, both NH_2-MIL-125(Ti) MOF (Figure 3 (c)) and Au nanoparticles (Figure 3 (e)) displayed spherical-like structure with approximate diameters of 80 and 100 nm, respectively. All the top (Figure 3 (g-j)) and cross-sectional view (Figure 3 (i-o)) FESEM images of the TNTAs-modified samples displayed good distribution and dispersion of the g-C_3N_4, MOF, RGO and Au over and between the tube wall revealing the effectiveness of the synthesis methods used in this study.

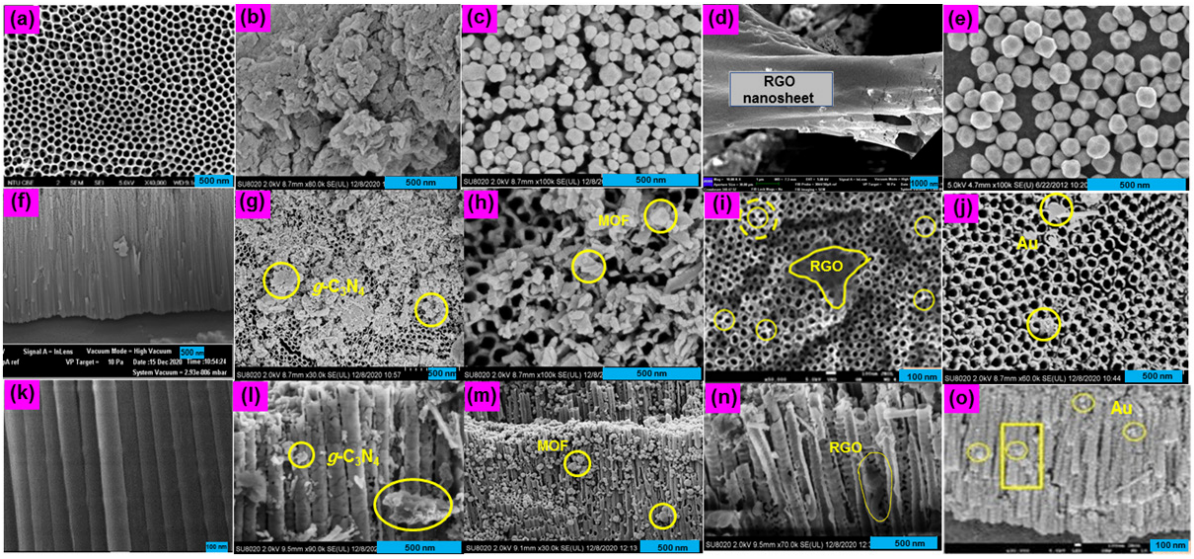

Figure 3. (a), (b), (c), (d) and (e) FESEM images of pure TNTAs, g-C_3N_4, MOF, RGO and Au, respectively, (f) cross-sectional view image of TNTAs, (g), (h), (i) and (j) top-view images of TNTAs/g-C_3N_4, TNTAs/MOF, TNTAs/RGO and TNTA/Au, respectively, (k), (l), (m), (n) and (o) cross-sectional view image of pure TNTAs, TNTAs/g-C_3N_4, TNTAs/MOF, TNTAs/RGO and TNTA/Au.

3.2. Photocatalytic CO_2 reduction

3.2.1. Photocatalytic performance of TNTAs

As shown in Figure 4, the pure TNTAs sample exhibited a continuous increasing production of CH_4 during the period of visible light irradiation which lasted for 4 h. However, a maximum CH_4 production rate of 62.66 µmol m^{-2} h^{-1} was exhibited after. The experimental investigation revealed the ability of TNTAs to convert the CO_2 gas into CH_4 in the presence of water after a serious of redox (reduction and oxidation) reactions. Compared to literature, Sim and co-workers [38] have reported the performance of pure TiO_2 nanotube arrays for photocatalytic reduction of CO_2 into CH_4 under visible light irradiation with a production rate of 1.28 µmol m^{-2} h^{-1}.
However, a CH_4 production of 2.88 µmol m^{-2} h^{-1} was achieved with the RGO/Pt–modified TiO_2 NTs. In 2018, Kar and co-workers [39] have also reported similar results for photocatalytic CO_2 reduction into CH_4 with an evolution rate of 67.9 µmol g^{-1} h^{-1} using flame annealed TiO_2 nanotubes under visible light.

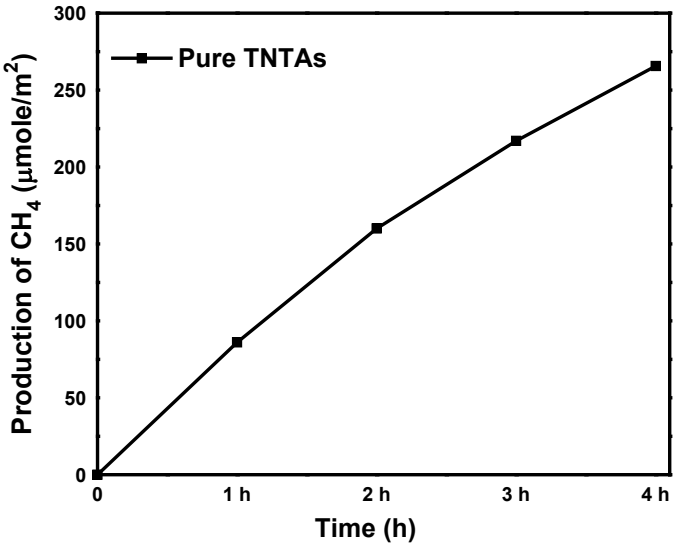

Figure 4 The amount of CH_4 produced over pure TNTAs after 4 h of light irradiation.

3.2.2. Effect of TNTAs modifications

The effect of modifying TNTAs with various materials was also studied (Figure 5). Obviously, the photocatalytic efficiency of TNTAs was improved with the modification of all used materials. The highest production rate (460.3 µmol m^{-2} h^{-1}) was observed with the g-C_3N_4-modified TNTAs sample, this represents about 7 times higher production compared to that of pure TNTAs. This was mainly attributed to the efficient heterojunction constructed between the g-C_3N_4-and TNTAs which suppressed the recombination of photo-generated electron-holes pairs.

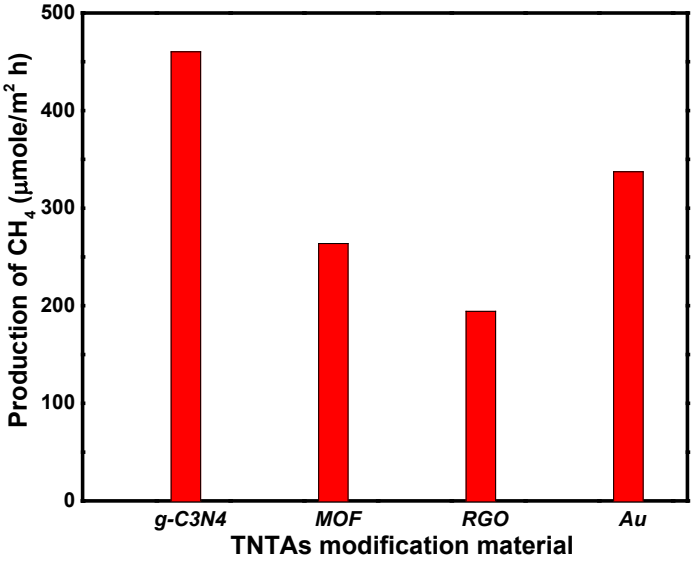

Figure 5. The effect of modifying TNTAs on the photocatalytic CO_2 reduction to CH_4.

Compared to pure TNTAs, the TNTAs/MOF, TNTAs/RGO and TNTA/Au composites exhibited higher results of 263.7, 194.2, 337.3 µmol m^{-2} h^{-1}, respectively. The NH_2-MIL-125(Ti) MOF is

known for its high ability for the adsorption of CO_2 gas which is beneficial in the photocatalytic process.

Table 2. A comparison of using different materials in modifying TNTAs for increasing the performance of photocatalytic CO_2 reduction into CH_4.

Co-catalyst	Synthesis method	Main role of co-catalyst	Production rate $\mu mol\ m^{-2}\ h^{-1}$	Enhancement compared to pure TNTAs
g-C_3N_4	Ultrasonic-assisted dying-deposition	Constructing efficient heterojunction to suppress charges recombination	460.3	7 times higher
MOF	Dying-deposition	Increasing CO_2 adsorption	263.7	4 times higher
RGO	Immersion-deposition	Improving charges separation and transfer	194.20	3 times higher
Au	Electrochemical-deposition	Increasing visible light harvesting	337.3	5 times higher

However, the addition of RGO provides good optoelectronic characteristics which can enhance the TNTAs performance while the Au nanoparticles can increase the ability of visible light harvesting in addition to its unique characteristic of LSPR (localized surface plasmon response) effect. Table 2 summarizes the comparison of effect of using different materials in modifying TNTAs for increasing the performance of photocatalytic CO_2 reduction into CH_4.

4. CONCLUSION

To summarize, this study investigated the use of TiO_2 nanotube arrays for the photo-conversion of CO_2 under visible light and in the presence of water. The TNTAs photocatalyst was modified with several materials through different synthesis methods. The effect of modifying TNTAs was investigated using both characterization analyses and experimental work. The maximum performance for the CO_2 reduction to CH_4 was exhibited with the TNTAs/g-C_3N_4 composite. This study provides new ideas for making and developing low-cost Ti metal-based nanomaterials which can be used in the future for recycling the CO_2 gas emissions into useful fuels.

Author Contributions: Riyadh Ramadhan Ikreedeegh (Methodology, Data collection, Writing-original draft, Conceptualization, Supervision, Reviewing and Editing), Muhammad Tahir (Supervision and Funding), and Mohamed Madi contributed to the Software and Reviewing.
Acknowledgments: Author would like to offer special thanks to United Arab Emirate University, Arabian Gulf Oil Company and the Libyan Advanced Center for Chemical Analysis for the support.
Funding: This research received no external funding.
Data Availability Statement: Data will be available upon request.
Conflicts of Interest: The authors declare that they have no conflict of interest.

REFERENCES

[1] Ikreedeegh, R.R. and M. Tahir, A critical review in recent developments of metal-organic-frameworks (MOFs) with band engineering alteration for photocatalytic CO_2 *reduction to solar fuels. J.* CO_2 *Util., 2021. 43: p. 101381.*

[2] Ikreedeegh, R.R., A Techno-Economical Evaluation Study for Upgrading Sarir Oil Refinery and Maximizing Gasoline Production. J. Chem. Petrol. Engin., 2023.

[3] Hossen, M.A., et al., Optimization of anodizing parameters for the morphological properties of TiO_2 nanotubes based on response surface methodology. Next Mater., 2024. 2: p. 100061.

[4] Ikreedeegh, R.R., et al., A comprehensive review on anodic TiO_2 nanotube arrays (TNTAs) and their composite photocatalysts for environmental and energy applications: Fundamentals, recent advances and applications. Coord. Chem. Rev., 2024. 499: p. 215495.

[5] Ikreedeegh, R.R., S. Tasleem, and M.A. Hossen, Facile fabrication of binary g-C_3N_4/NH_2-MIL-125 (Ti) MOF nanocomposite with Z-scheme heterojunction for efficient photocatalytic H2 production and CO_2 reduction under visible light. Fuel, 2024. 360: p. 130561.

[6] Gao, J., et al., Oxygen vacancy self-doped black TiO_2 nanotube arrays by aluminothermic reduction for photocatalytic CO_2 reduction under visible light illumination. Journal of CO_2 Utilization, 2020. 35: p. 205-215.

[7] Ikreedeegh, R.R. and M. Tahir, Ternary nanocomposite of NH_2-MIL-125(Ti) MOF-modified TiO_2 nanotube arrays (TNTs) with GO electron mediator for enhanced photocatalytic conversion of CO_2 to solar fuels under visible light. Journal of Alloys and Compounds, 2023. 969: p. 172465.

[8] Yu, Y., et al., Pd quantum dots loading Ti3+,N co-doped TiO_2 nanotube arrays with enhanced photocatalytic hydrogen production and the salt ions effects. Applied Surface Science, 2021. 540: p. 148239.

[9] Cao, D., et al., Solvothermal synthesis and enhanced photocatalytic hydrogen production of Bi/Bi2MoO6 co-sensitized TiO_2 nanotube arrays. Separation and Purification Technology, 2020. 250: p. 117132.

[10] Hou, J., et al., Constructing Ag2O nanoparticle modified TiO_2 nanotube arrays for enhanced photocatalytic performances. Journal of Alloys and Compounds, 2020. 849: p. 156493.

[11] Zhou, D., et al., Improved visible light photocatalytic activity on Z-scheme g-C_3N_4 decorated TiO_2 nanotube arrays by a simple impregnation method. Materials Research Bulletin, 2020. 124: p. 110757.

[12] Dai, K., et al., Efficient visible-light-driven splitting of water into hydrogen over surface-fluorinated anatase TiO_2 nanosheets with exposed {001} facets/layered CdS–diethylenetriamine nanobelts. ACS sustainable chemistry and engineering, 2018. 6(10): p. 12817-12826.

[13] Ke, X., et al., Construction of flourinated-TiO_2 nanosheets with exposed {001} facets/CdSe-DETA nanojunction for enhancing visible-light-driven photocatalytic H2 evolution. Ceramics International, 2020. 46(1): p. 866-876.

[14] Tahir, B., M. Tahir, and N.S. Amin, Gold–indium modified TiO_2 nanocatalysts for photocatalytic CO_2 reduction with H2 as reductant in a monolith photoreactor. Applied Surface Science, 2015. 338: p. 1-14.

[15] Jun, Y., J.H. Park, and M.G. Kang, The preparation of highly ordered TiO_2 nanotube arrays by an anodization method and their applications. Chemical communications, 2012. 48(52): p. 6456-6471.

[16] Roy, P., S. Berger, and P. Schmuki, TiO_2 nanotubes: synthesis and applications. Angewandte Chemie International Edition, 2011. 50(13): p. 2904-2939.

[17] Bu, T., et al., Organic/inorganic self-doping controlled crystallization and electronic properties of mixed perovskite solar cells. Journal of Materials Chemistry A, 2018. 6(15): p. 6319-6326.

[18] Yilleng, M.T., et al., Batch to continuous photocatalytic degradation of phenol using TiO_2 and Au-Pd nanoparticles supported on TiO_2. Journal of Environmental Chemical Engineering, 2018. 6(5): p. 6382-6389.

[19] Mazierski, P., et al., Photocatalytically active TiO_2/Ag_2O nanotube arrays interlaced with silver nanoparticles obtained from the one-step anodic oxidation of Ti–Ag alloys. ACS Catalysis, 2017. 7(4): p. 2753-2764.

[20] Moon, S.Y., et al., Plasmonic hot carrier-driven oxygen evolution reaction on Au nanoparticles/ TiO_2 nanotube arrays. Nanoscale, 2018. 10(47): p. 22180-22188.

[21] Altomare, M., et al., H2 and O2 photocatalytic production on TiO_2 nanotube arrays: Effect of the anodization time on structural features and photoactivity. Applied Catalysis B: Environmental, 2013. 136-137: p. 81-88.

[22] Ikreedeegh, R.R. and M. Tahir, Facile fabrication of well-designed 2D/2D porous g-C_3N_4–GO nanocomposite for photocatalytic methane reforming (DRM) with CO_2 towards enhanced syngas production under visible light. Fuel, 2021. 305: p. 121558.

[23] Ikreedeegh, R.R. and M. Tahir, Indirect Z-scheme heterojunction of NH_2-MIL-125 (Ti) MOF/ g-C_3N_4 nanocomposite with RGO solid electron mediator for efficient photocatalytic CO_2 reduction to CO and CH_4. J. Environ. Chem. Eng., 2021: p. 105600.

[24] Hu, J., J. Ding, and Q. Zhong, In situ fabrication of amorphous TiO_2/NH_2-MIL-125(Ti) for enhanced photocatalytic CO_2 into CH_4 with H2O under visible-light irradiation. J. Colloid Interface Sci., 2020. 560: p. 857-865.

[25] Azam, M.U., et al., In-situ synthesis of TiO_2/La2O2CO3/rGO composite under acidic/basic treatment with La3+/Ti3+ as mediators for boosting photocatalytic H2 evolution. Int. J. Hydrog. Energy, 2019. 44(42): p. 23669-23688.

[26] Khatun, F., et al., Plasmonic enhanced Au decorated TiO_2 nanotube arrays as a visible light active catalyst towards photocatalytic CO_2 conversion to CH_4. J. Environ. Chem. Eng., 2019. 7(6): p. 103233.

[27] Hossen, M.A., et al., Enhanced photocatalytic CO_2 reduction to CH_4 using novel ternary photocatalyst RGO/Au-TNTAs. Energies, 2023. 16(14): p. 5404.

[28] Wu, J., et al., Preparation of Al–O-Linked Porous-g-C_3N_4/TiO_2-Nanotube Z-Scheme Composites for Efficient Photocatalytic CO_2 Conversion and 2, 4-Dichlorophenol Decomposition and Mechanism. ACS Sustain. Chem. Eng., 2019. 7(18): p. 15289-15296.

[29] Phromma, S., et al., Effect of Calcination Temperature on Photocatalytic Activity of Synthesized TiO_2 Nanoparticles via Wet Ball Milling Sol-Gel Method. Appl. Sci., 2020. 10(3): p. 993.

[30] Liu, L., et al., Photocatalytic CO_2 reduction with H2O on TiO_2 nanocrystals: Comparison of anatase, rutile, and brookite polymorphs and exploration of surface chemistry. ACS Catal., 2012. 2(8): p. 1817-1828.

[31] Kar, P., et al., High rate CO_2 photoreduction using flame annealed TiO_2 nanotubes. Appl. Catal. B, 2019. 243: p. 522-536.

[32] Gao, Z., et al., Construction of heterostructured g-C_3N_4@ TiATA/Pt composites for efficacious photocatalytic hydrogen evolution. Int. J. Hydrogen Energy, 2019. 44(45): p. 24407-24417.

[33] Wang, Y., et al., Novel g-C_3N_4 assisted metal organic frameworks derived high efficiency oxygen reduction catalyst in microbial fuel cells. J. Power Sources, 2020. 450: p. 227681.

[34] Kumar, S., et al., Ag nanoparticles–anchored reduced graphene oxide catalyst for oxygen electrode reaction in aqueous electrolytes and also a non-aqueous electrolyte for Li–O2 cells. Phys. Chem. Chem. Phys., 2014. 16(41): p. 22830-22840.

[35] Kumar, A., A.M. Sadanandhan, and S.L. Jain, Silver doped reduced graphene oxide as a promising plasmonic photocatalyst for oxidative coupling of benzylamines under visible light irradiation. New J Chem, 2019. 43(23): p. 9116-9122.

[36] Wei, C., et al., MOF-derived mesoporous g-C_3N_4/TiO_2 heterojunction with enhanced photocatalytic activity. Catal. Lett., 2021. 151: p. 1961-1975.

[37] Zhang, X., et al., Construction of NH_2-MIL-125(Ti)/CdS Z-scheme heterojunction for efficient photocatalytic H2 evolution. J. Hazard. Mater., 2021. 405: p. 124128.

[38] Sim, L.C., et al., Rapid thermal reduced graphene oxide/Pt–TiO_2 nanotube arrays for enhanced visible-light-driven photocatalytic reduction of CO_2. Applied Surface Science, 2015. 358: p. 122-129.

[39] Kar, P., et al., High rate CO_2 photoreduction using flame annealed TiO_2 nanotubes. Applied Catalysis B: Environmental, 2019. 243: p. 522-536.